JGR Atmospheres

RESEARCH ARTICLE
10.1029/2023JD038891

On the Role of Continuing Currents in Lightning-Induced Fire Ignition

Francisco J. Pérez-Invernón[1], Jose V. Moris[2], Francisco J. Gordillo-Vázquez[1], Martin Füllekrug[3], Gianni Boris Pezzatti[4], Marco Conedera[4], Jeff Lapierre[5], and Heidi Huntrieser[6]

[1]Instituto de Astrofísica de Andalucía (IAA), CSIC, Granada, Spain, [2]Department of Agricultural, Forest and Food Sciences (DISAFA), University of Turin, Grugliasco, Italy, [3]Department of Electronic and Electrical Engineering, Center for Space, Atmospheric and Oceanic Science, University of Bath, Bath, UK, [4]WSL Swiss Federal Institute for Forest Snow and Landscape Research, Insubric Ecosystems Research Group, Cadenazzo, Switzerland, [5]Earth Networks, Germantown, MD, USA, [6]Deutsches Zentrum für Luft- und Raumfahrt, Institut für Physik der Atmosphäre, Oberpfaffenhofen, Germany

Abstract Lightning flashes are an important source of wildfires worldwide, contributing to the emission of trace gases to the atmosphere. Based on experiments and field observations, continuing currents in lightning have since a long time been proposed to play a significant role in the ignition of wildfires. However, simultaneous detections of optical and radio signals from fire-igniting lightning confirming the role of continuing currents in igniting wildfires are rare. In this work, we first analyze the optical signal of the lightning-ignited wildfires reported by the Geostationary Lightning Mapper over the Contiguous United States (CONUS) during the summer of 2018, and we then analyze the optical and the Extremely Low Frequency signal of a confirmed fire-igniting lightning flash in the Swiss Alps. Despite data uncertainties, we found that the probability of ignition of a lightning flash with Continuing Current (CC) lasting more than 10 ms is higher than that of cloud-to-ground lightning in CONUS. Finally, we confirm the existence of a long CC (lasting about 400 ms) associated with a long-lasting optical signal (lasting between 2 and 4 s) of a video-recorded fire-igniting lightning flash.

Plain Language Summary Lightning plays a significant role in causing natural fires. Previous studies have found that a specific type of lightning, known as continuing current lightning (CC), has a higher likelihood of igniting fires. CC lightning refers to a phenomenon where electrical charge continues to flow through the channel for extended periods of tens or hundreds of milliseconds, possibly leading to elevated vegetation temperatures. In our research, we used the optical lightning detections provided by the Geostationary Lightning Mapper to estimate the probability of wildfires associated with both normal lightning and CC lightning across the United States. To gain further insights, we employed a ground camera video and analyzed extremely low-frequency radio signals to meticulously examine the duration of CC in a lightning strike that ignited a fire in the Alps. The findings of our study demonstrate that the probability of fire occurrence is higher when CC lightning is involved compared to typical lightning strikes. This highlights the importance of understanding the characteristics of lightning and its varying impacts on fire risk assessment.

Key Points:

- The probability of wildfire ignition by cloud-to-ground lightning is larger for flashes with Continuing Current (CC)
- The variation of the lightning ignition efficiency of lightning with CC suggest a significant influence of other factors
- The analysis of one single lightning-ignited fire in the Alps confirms the presence of a lightning with a long CC

Correspondence to:
F. J. Pérez-Invernón,
fjpi@iaa.es

Citation:
Pérez-Invernón, F. J., Moris, J. V., Gordillo-Vázquez, F. J., Füllekrug, M., Pezzatti, G. B., Conedera, M., et al. (2023). On the role of continuing currents in lightning-induced fire ignition. *Journal of Geophysical Research: Atmospheres*, *128*, e2023JD038891. https://doi.org/10.1029/2023JD038891

Received 14 MAR 2023
Accepted 7 OCT 2023

Author Contributions:
Conceptualization: Francisco J. Pérez-Invernón, Jose V. Moris, Francisco J. Gordillo-Vázquez, Heidi Huntrieser
Data curation: Francisco J. Pérez-Invernón, Jose V. Moris, Francisco J. Gordillo-Vázquez, Martin Füllekrug, Gianni Boris Pezzatti, Marco Conedera, Jeff Lapierre, Heidi Huntrieser
Formal analysis: Francisco J. Pérez-Invernón, Jose V. Moris, Martin Füllekrug, Gianni Boris Pezzatti, Marco Conedera, Jeff Lapierre, Heidi Huntrieser
Funding acquisition: Francisco J. Pérez-Invernón
Investigation: Francisco J. Pérez-Invernón, Jose V. Moris, Francisco J. Gordillo-Vázquez, Martin Füllekrug, Jeff Lapierre, Heidi Huntrieser

1. Introduction

Wildfires are a key element of the Earth system, producing significant emissions of carbon dioxide, methane, nitrous oxide, carbon monoxide, carbonaceous aerosols, and other gases including non-methane volatile organic compounds (Akagi et al., 2011; Huntrieser et al., 2016; Zheng et al., 2023). Lightning is the main natural cause of wildfire ignition worldwide (Komarek, 1964; Latham & Williams, 2001; Pyne et al., 1998) and it represents the major ignition source in low populated areas (Calef et al., 2017; Coogan et al., 2020). Projections of Lightning-Ignited Wildfires (LIW) under climate change show a possible change of pattern (Krause et al., 2014; Pérez-Invernón et al., 2023) and a significant increase in some areas, such as in polar regions (Chen et al., 2021; Zheng et al., 2023).

LIW consist of three phases, i.e., ignition (fire triggering), survival (smoldering combustion) and arrival (flaming combustion) (Anderson, 2002, an references therein). The *ignition phase* occurs when a lightning flash strikes vegetation transporting a significant amount of electrical charge and causing ignition. The *survival* and *arrival phases* account for the emergence and spread of the fire, which are determined by the meteorological conditions

Methodology: Francisco J. Pérez-Invernón, Jose V. Moris, Jeff Lapierre, Heidi Huntrieser
Project Administration: Francisco J. Pérez-Invernón
Resources: Francisco J. Pérez-Invernón
Software: Francisco J. Pérez-Invernón, Francisco J. Gordillo-Vázquez, Martin Füllekrug
Supervision: Jose V. Moris, Francisco J. Gordillo-Vázquez, Jeff Lapierre, Heidi Huntrieser
Validation: Francisco J. Pérez-Invernón, Jose V. Moris, Francisco J. Gordillo-Vázquez, Martin Füllekrug, Gianni Boris Pezzatti, Marco Conedera, Jeff Lapierre, Heidi Huntrieser
Visualization: Francisco J. Pérez-Invernón, Jose V. Moris, Heidi Huntrieser
Writing – original draft: Francisco J. Pérez-Invernón, Jose V. Moris, Heidi Huntrieser
Writing – review & editing: Francisco J. Pérez-Invernón, Jose V. Moris, Francisco J. Gordillo-Vázquez, Martin Füllekrug, Gianni Boris Pezzatti, Marco Conedera, Jeff Lapierre, Heidi Huntrieser

and the fuel availability and moisture. Wildfires ignited by lightning are reported only when the arrival phase is reached and they become detectable by local fire alarm/monitoring systems or satellite-based instruments (Justice et al., 2002; Moris et al., 2023). Therefore, research focused on the ignition phase is scarce.

There are differences between lightning-induced fires and anthropogenic fires that justify the need to study them separately. For example, Hantson et al. (2022) reported that human-caused wildfires in California during 2012–2018 evolved to more extreme fires than lightning-ignited fires. On the contrary, Rodrigues et al. (2023) revealed that lightning emerged as the primary cause for extreme wildfires in Southwest Europe in 2022, contributing to approximately 38% of all extreme wildfires, despite constituting only around 5% of the total wildfire count.

Lightning flashes containing a Continuing Current (CC) can transport more electrical charge that impulsive lightning flashes with no CC. For this reason, lightning flashes with CC have been proposed to be the main precursors of lightning ignitions (Anderson, 2002, an references therein). This hypothesis is supported by multiple laboratory experiments (e.g., Feng et al., 2019; McEachron & Hagenguth, 1942; H. Zhang et al., 2021) and some field and satellite-based observations (e.g., D. M. Fuquay et al., 1967; D. Fuquay et al., 1972; Latham & Williams, 2001; Pérez-Invernón et al., 2021, 2023). However, the characteristics of the electromagnetic signals produced by continuing currents prevent a continuous monitoring of their occurrence by using ground-based lightning location systems, making it difficult to quantify the number of wildfires caused by CC. The near-field component of the electromagnetic field transports the vast majority of the energy emitted by continuing currents, decreasing with distance following an inverse-cubic law (Pérez-Invernón et al., 2016; Rakov & Uman, 2003). Lightning location systems, commonly composed of Very Low-Frequency (VLF) and Low Frequency (LF) sensors that are sensitive to the far-field component of the electromagnetic field (Nag et al., 2015) have a low detection efficiency of the CC of lightning, typically recorded at frequencies <1 kHz. Alternatively, Extremely Low Frequency (ELF) sensors that are sensitive to the near-field component of the electromagnetic or optical sensors reporting the continuous duration of the flashes (Adachi et al., 2009; Bitzer, 2017; Fairman & Bitzer, 2022; Montanyà et al., 2021) are necessary to detect CC in lightning discharges. To the best of our knowledge, the only reports of simultaneous measurements of optical and ELF signals from fire-igniting lightning were published by D. M. Fuquay et al. (1967) and D. Fuquay et al. (1972) in western Montana forests, indicating that flashes with long CC (CC lasting more than 40 ms) could be the main igniting source of lightning-induced wildfires. There are still noteworthy questions about the key features of lightning flashes that favor the ignition of lightning-induced wildfires. For example, what is the role of CC in the probability ignition? What are the optical and electrical characteristics of the CC that ignite reported wildfires?

The Geostationary Lightning Mapper (GLM) can provide continuous measurements of the optical signal emitted by lightning in the Americas, as well as in some parts of the Pacific Ocean and the Atlantic Ocean. Fairman and Bitzer (2022) have recently developed a new method to classify lightning flashes with CC lasting more than 10 ms derived from the 777 nm optical characteristics of flashes reported by GLM. They reported that in 2018, 13.3% of all flashes detected by GLM in CONUS with no degraded flags (see below) contained continuing currents. Note that Degraded flashes are those that are composed of events that occur out of order temporally, consist of more than 101 groups, or exceed a duration of 2,998 ms (Fairman & Bitzer, 2022). Fairman and Bitzer (2022) reported that during the summer months and over land, the ratio of lightning flashes with continuing currents to total lightning flashes reaches its minimum at nearly 10%. Additionally, Pérez-Invernón et al. (2023) searched for lightning candidates with CC for wildfires in the Contiguous United States (CONUS) by using a spatio-temporal threshold, reporting that more than 10% of lightning-induced wildfires can be associated with lightning with CC. Apart from GLM, the Lightning Mapping Imager aboard the Feng-Yun-4 satellite (FY-4) since 2018 (Yang et al., 2017), and the Meteosat Third Generation geostationary satellites of the EUropean organization for the exploitation of METeorological SATellites equipped with a lightning imager launched on 13 December 2022 (Stuhlmann et al., 2005), will also provide continuous geostationary observations of lightning that can serve to develop a global climatology of lightning flashes with CC and to monitor their relationships with fire ignitions.

In this work, we investigate the role of CC in the ignition of lightning-induced wildfires by using lightning data from GLM, fire data provided by the U.S. Department of Agriculture (Short, 2021; Wright et al., 2011) during 2018, and vegetation data from the Moderate Resolution Imaging Spectroradiometer (MODIS) imagery and Forest Inventory and Analysis (FIA) plot data (Ruefenacht et al., 2008). We extend the analysis of Pérez-Invernón et al. (2023) by comparing the lightning candidates with and without CC and by introducing an estimation of the total number of cloud-to-ground lightning candidates based on the climatology provided by Medici et al. (2017),

who took into account the possible multiyear variation. We provide the holdover time and spatial distance between wildfires and lightning candidates from GLM data. In addition, we explore the optical and electrical characteristics of a flash with CC able to ignite a reported wildfire. With this purpose, we investigate both the optical and ELF signal of a fire-igniting lightning flash recorded on 21 July 2021 by a camera in the Valais (Switzerland) so that we can examine in detail the duration of fire-igniting lightning discharges. To the best of our knowledge, this event is the first fire-igniting lightning simultaneously recorded by a camera and an ELF sensor in Europe. This particular event allows us to investigate the optical characteristics of fire-producing lightning in Europe when the MTG-LI (Stuhlmann et al., 2005) has just been launched (13 December 2022).

2. Data and Methodology

2.1. Lightning Data

We used lightning data over CONUS between 15 May 2018 and 31 August 2018 provided by the GLM, aboard the Geostationary Operational Environmental Satellite-16 (GOES-16) (Goodman et al., 2013) since 2017 and aboard the GOES-17 since 2018. The GLM is a Charge-Coupled Device imager with narrow spectral band filters centered on the atomic oxygen line 777.4 nm that are usually associated with lightning (Kieu et al., 2021; Orville, 1968; Pérez-Invernón, Gordillo-Vázquez, et al., 2022). The GLM can provide continuous measurements of the optical signal emitted by lightning in the Americas, some parts of the Pacific Ocean and the Atlantic Ocean. The GLM pixel sizes exhibit a range of approximately 8 km across the majority of its field of view (FOV), which gradually increases to around 14 km at its edges (Goodman et al., 2013). The clustering algorithm groups events (pixels illuminated during 2 ms) into groups and considers groups of a single flash if they fall within 330 ms and less than 16.5 km of each other, and using the centroid of the events coordinates as the location of the groups (Goodman et al., 2013; Mach et al., 2007; Peterson, 2019). Groups detected by GLM can be associated with the strokes detected by ground-based networks. The algorithm that cluster groups into flashes estimates the coordinates of each flash as the centroid of the groups weighted by their energy. The optical signature of lightning measured by GLM is usually scattered and reflected by clouds above the lightning channel (Montanyà et al., 2021; Pérez-Invernón, Gordillo-Vázquez, et al., 2022), causing the illumination of a large area of clouds. Flashes with CC observed by GLM and confirmed with ELF sensors (Montanyà et al., 2021, 2022) showed that the illuminated area can extend further than 0.5° from the location of the grounding-point of the flash. Nevertheless, the activity of the groups is more frequent and intense near the point where the lightning strikes the ground (Montanyà et al., 2021; Pérez-Invernón, Gordillo-Vázquez, et al., 2022), suggesting that taking the position of the flash as the centroid of the groups weighted by their energy is appropriate to search for lightning candidates for wildfires when dealing with lightning with CC. On the other hand, using the position of individual groups to determine the best candidate group has the disadvantage that the vast majority of pulses detected by GLM corresponds to Intra-Cloud (IC) pulses.

The GLM product does not provide information about the type of the lightning flashes, i.e, IC or Cloud to Ground (CG). However, Ringhausen et al. (2021) have demonstrated that a classification method can be used to distinguish between IC and CG flashes based on the optical characteristics of lightning flashes detected by GLM. In addition, Peterson and Mach (2022) have developed a method to acquire height information from GLM data.

We used the method developed by Fairman and Bitzer (2022) to classify lightning flashes with CC lasting more than 10 ms from GLM measurements based on the characteristics of the measured optical signals. For each flash we identified the maximum sample of time-contiguous groups and estimated the maximum distance between two groups in the sample, the maximum group footprint, the maximum group optical energy, the maximum number of time-contiguous groups, the median group optical energy and the total group optical energy. Then, we applied the logistic regression model of Fairman and Bitzer (2022, Table 1) by assuming that flashes with CC had probabilities at or above a 0.33 threshold, which implies a probability of detection of lightning with CC of 78% and a false alarm rate of 6%.

Furthermore, we used lightning data from the Earth Networks Global Lightning Network (ENGLN), the lightning detection network (LINET) of Nowcast GmbH and the ELF sensor located at the Eskdalemuir Observatory in Scotland (Musur & Beggan, 2019) to analyze a single lightning-ignited wildfire in the Swiss Alps. The ENGLN is a global network composed of VLF/LF sensors that provide the position, time of occurrence, polarity, and peak current of lightning strokes with, at the time of these events, a median location uncertainty of 215 m as observed

in Florida U.S.A. (Zhu et al., 2015, 2022). In turn, LINET is a lightning network with VLF and LF sensors located over four continents (including 65 sensors in Europe) monitoring the occurrence of lightning strokes with an average location uncertainty of 150 m (Betz et al., 2009).

2.2. Fire Data

Fire data, including the cause of the wildfires, are reported by the U.S. Department of Agriculture (Short, 2021; Wright et al., 2011). The coordinates of the wildfires are reported with a minimum spatial accuracy of 1-square mile (i.e., 2.6 km^{-2}), together with the date and time of detection. As in Pérez-Invernón et al. (2023), we have extracted 5,860 LIW taking place over CONUS between 1 June 2018 and 31 August 2018.

The investigated lightning-ignited fire in the Alps was extracted from the forest fire database of Switzerland "Swissfire" (Moris et al., 2020; Pezzatti et al., 2019). In particular, this event took place on 21 July 2021 in the Valais (Switzerland) 615,307 m E and 126,417 m N CH 1,903 coordinates (7.64°E and 46.29°N). The flash was recorded at a frequency rate of 30 frames per second by the Complementary Metal Oxide Semiconductor (CMOS) camera of a Samsung Galaxy S8 Plus smartphone between 21 and 22 hr (UTC-0). According to the video (Berckum et al., 2023), the fire-igniting lightning flash was followed by a second flash that took place less than a second after its onset.

2.3. Vegetation Data and Ecological Regions

The Lightning Ignition Efficiency (LIE) is defined as the number of wildfires ignited per lightning (Pineda et al., 2022; Podur et al., 2003). The spatial distribution of the ratio of lightning with CC to total lightning is not homogeneous across CONUS (Fairman & Bitzer, 2022). Therefore, comparing the LIE of total flashes with the LIE of flashes with CC at a continental scale may be misleading. We calculated the LIE for all flashes, CG flashes, and flashes with CC separately over different forest types and ecological regions to analyze the role of continuing currents in the ignition of wildfires. Distinguishing between forest types may help to reduce the effect of the type of vegetation in the probability of ignition by lightning, while distinguishing between ecological regions may serve us to partially remove the contribution of climate (Pérez-Invernón, Huntrieser, & Moris, 2022). Therefore, we used a 250 m resolution map of the United States forest types (Ruefenacht et al., 2008) and a map of ecological regions to investigate the LIE in the main forest types of CONUS (Podur et al., 2003). The forest type map was generated from MODIS imagery and FIA plot data, and classifies the forest area into discrete classes based on the dominant tree species (Ruefenacht et al., 2008). In turn, the map of ecological regions follows a holistic approach based on the major components of ecosystems, including air, water, land and biota (Commission for Environmental Cooperation, 1997 (Revised 2006)). We assigned a forest type and an ecological region to each fire using their coordinates. To accurately account for the minimal spatial uncertainty introduced by GLM pixels (∼8 km and increasing to ∼14 km at the edge of the full-disk view (Marchand et al., 2019)), we assigned to each flash the predominant forest type and ecological region within a 4 km radius from its coordinates.

2.4. Search for GLM Lightning Candidates

Establishing a one-by-one relationship between LIW and lightning flashes is complex because the detection efficiency of GLM in CONUS ranges between 43% and 90% (Marchand et al., 2019) depending on the solar zenith angle and the charge structure of the thunderstorm. However, there is no indication that the variability of the DE of GLM could affect the total number of lightning with and without continuing currents differently (Fairman & Bitzer, 2022). In addition, the official GLM product does not provide information about the type of lightning, that is, IC or CG, and the position and time of the flashes, the groups, and the fires can include errors that can influence the matching between them. For these reasons, we used the proximity index A proposed by Larjavaara et al. (2005) to search for the most probable lightning candidates and to find the parent thunderstorm of each fire,

$$A = \left(1 - \frac{T}{T_{\max}}\right) \times \left(1 - \frac{D}{D_{\max}}\right), \quad (1)$$

where D is the distance between the reported fire location and the lightning flash or group, and T is the time between fire ignition and detection, also known as holdover time (Moris et al., 2023; Wotton & Martell, 2005).

Parameters (T_{max}) and (D_{max}) correspond to the maximum holdover time and distance between a fire and a lightning discharge to consider the latter as the potential cause of ignition. A distance of $D_{max} = 10$ km is often applied in the literature to account for possible large location errors in fire and lightning data reported by lightning location systems (Larjavaara et al., 2005; Moris et al., 2020; Pérez-Invernón et al., 2021; Schultz et al., 2019; Wotton & Martell, 2005). However, a threshold $D_{max} = 10$ km could be considered too small for flashes coordinates reported by GLM, as the uncertainty of the position of flashes reported by GLM is larger than in the case of lightning location systems. Methods to match space-based optical signal of lightning and lightning location systems usually set a maximum distance of 25 km for the flash level (Bitzer et al., 2016; Pérez-Invernón, Huntrieser, Erbertseder, et al., 2022; Rudlosky et al., 2017). Therefore, we use D_{max} values ranging between 10 and 25 km in order to estimate the sensitivity of our results. Using $T_{max} = 14$ days is a conservative approach that allows us to include a representative sample of LIW by discarding fires with long (>14 days) holdover durations that might have been erroneously labeled as natural fires (Schultz et al., 2019). Thus, we did not include in subsequent analysis fires for which no lightning discharges were detected within the proposed spatio-temporal windows.

As an alternative method to assess the robustness of the results, we have searched for lightning candidates by using the groups detected by GLM. For each fire, we calculated the A-index for all groups within a 10 km radius and up to 14 days before the detection. Subsequently, we selected lightning flashes as candidates if they included any of the candidate groups. This approach may include numerous groups generated by IC leader activity, but it allows us to evaluate the limitations of our study.

We explored the role of continuing currents in lightning-induced fire ignitions by using the proximity index A of all the possible flash candidates. The GLM detects total lightning (CG and IC), while only CG lightning can ignite a fire. Therefore, we cannot assume that the lightning candidate with maximum proximity index is the only possible candidate. Instead, we search for all the possible candidates for each fire with a proximity index A greater than 0. We then calculated, for each single fire, the distribution of values of the proximity index A of all the flashes candidates. We considered that the fire may have been ignited by a flash with CC if there is at least one CC flash with a proximity index above a given percentile of the index A values. In particular, we used different minimum percentiles ranging between the 0th and the 100th percentile to test the robustness of the results.

2.4.1. Lightning Candidate for the Recorded Lightning-Ignited Wildfire

A fire-igniting lightning flash has been recorded on 21 July 2021 between 21 and 22 hr (UTC-0) in the Valais (Switzerland) by a camera operating at 30 frames per second. Based on this video, we searched for the candidate stroke manually by using as reference the two flashes recorded in the video. The exact timing of the fire-igniting lightning stroke is needed in order to investigate its ELF signature. We used lightning measurements from lightning location networks to establish the timing of the stroke. We inspected all the ENGLN and LINET strokes reported between 21 and 22 hr (UTC-0) within 10 km distance around the position of the fire and selected the pair of CG strokes with the same time between strokes as the two flashes recorded in the video. We calculated the Charge Moment Change (CMC) of the discharge from the ELF signal by following Füllekrug (2000), Füllekrug and Constable (2000), and Füllekrug et al. (2006). With this purpose, we first calculate the transfer function as

$$T(\omega, \vartheta) = \sum_n \frac{l(2n+1)P_n^1(\cos\vartheta)}{4\pi a^3 h_1(\omega)\varepsilon_0(\omega-\omega_n)(\omega-\omega_n^*)}, \quad (2)$$

where l is the lightning flash length, assumed to be 7 km. ω is the frequency of the radio wave, ϑ is the angular distance between the flash and the sensor, $h_1(\omega)$ is the conduction boundary (50 km), and $P_n^1(\cos\vartheta)$ are the associated Legendre polynomials of degree n and order $m = 1$ on a spheroidal earth with radius $a = 6{,}371$ km. The complex modal frequency ω_n is calculated according to Füllekrug (2000) and by considering the ionospheric reflection height at 100 km. The lightning current $I(\omega)$ is then calculated as

$$I(\omega) = \frac{B(\omega, \vartheta)}{T(\omega, \vartheta)}, \quad (3)$$

where $B(\omega, \vartheta)$ is the recorded magnetic field. Finally, the CMC is calculated by integration of $I(\omega)$ and assuming 7 km flash length.

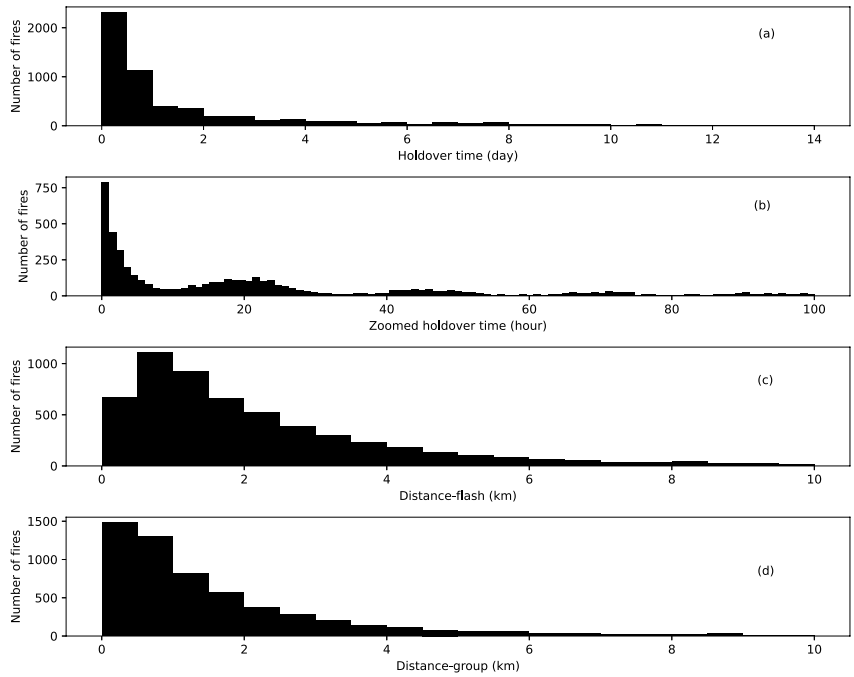

Figure 1. Holdover time in days (a), holdover time in hours for the first 100 hr (b) and distance between each fire and the most probable (maximum A index) lightning flash candidate (c) and group candidate (d) using D_{max} = 10 km.

2.4.2. Lightning Ignition Efficiency Estimate

We calculate the LIE of total lightning, CG lightning and lightning with CC in different forest types and ecological regions. The LIE of total lightning is estimated as the ratio of the total number of lightning-induced wildfires to total flashes. The LIE of CG lightning in each forest type and ecological region is estimated from total lightning by using the mapped climatological IC fraction reported by Medici et al. (2017, Figure 6) over CONUS during more than 2 decades. We calculated the average IC fraction and the standard deviation in each forest type and ecological region. We used the total number of flashes reported by GLM and the average IC fraction ± the standard deviation of the IC fraction to calculate the total number of CG lightning and an uncertainty measure. Finally, the LIE of lightning with CC is calculated by assuming that a wildfire was ignited by a flash with CC only if there is at least one lightning candidate with CC with a proximity index A above the 95th or the 99th percentile by using a holdover of T_{max} = 14 days and a spatial matching constraint D_{max} = 10 km. We selected the 95th and the 99th percentiles as thresholds for identifying wildfires ignited by flashes with CC to reduce the possibility that flashes with CC were within 10–25 km and 14 days from the fire by pure chance when the number of lightning candidates is high (Section 3.1.1). We did not include in our analysis forest types and ecological regions where the total number of fires is too low to be significant. In particular, we limited our analysis to forest types and ecological regions containing at least 2% of the reported total number of natural fires.

3. Results

3.1. Characteristics of Fire-Igniting Lightning From GLM Measurements

3.1.1. Lightning Candidates and Continuing Currents

We found a total number of 1,033,318 and 6,085,706 flashes candidates for 5,860 fires labeled as LIW by using D_{max} values of 10 and 25 km, respectively, and T_{max} = 14 days. In particular, we found at least one lightning candidate for 5,585 (95%) and 5,731 (98%) fires by using D_{max} values of 10 and 25 km and the flashes coordinates, respectively. In turn, we found 10,683,999 groups candidates by using D_{max} values of 10 km and T_{max} = 14 days. We found at least one group candidate for 5,634 (96%) fires by using D_{max} = 10 km and the groups coordinates.

Figure 1 shows the holdover time (a, b) and the distance (c) between each fire and the most probable (maximum A index) lightning flash candidate by using D_{max} = 10 km. As reported by Pérez-Invernón, Huntrieser, and

Table 1
Total Number of Lightning-Ignited Wildfires With At Least One Flash With Continuing Current Candidate Lasting More Than 10 ms Above a Given Percentile of Proximity Index A Among the Lightning Candidates, by Using Two Different Values of D_{max}

	Flash-based search		Group-based search
Percentile	D_{max} = 10 km 5,585 LIW	D_{max} = 25 km 5,731 LIW	D_{max} = 10 km 5,634 LIW
0th percentile	4,954 (89%)	5,669 (99%)	4,864 (86%)
10th percentile	4,844 (87%)	5,557 (97%)	4,754 (84%)
20th percentile	4,774 (86%)	5,532 (97%)	4,703 (83%)
30th percentile	4,667 (84%)	5,506 (96%)	4,631 (82%)
40th percentile	4,566 (82%)	5,470 (95%)	4,567 (81%)
50th percentile	4,453 (80%)	5,428 (95%)	4,455 (79%)
60th percentile	4,264 (76%)	5,369 (94%)	4,301 (76%)
70th percentile	3,981 (71%)	5,280 (92%)	4,085 (73%)
80th percentile	3,615 (65%)	5,079 (89%)	3,776 (67%)
90th percentile	2,880 (52%)	4,628 (81%)	3,237 (57%)
95th percentile	2,218 (40%)	3,999 (70%)	2,651 (47%)
99th percentile	1,180 (21%)	2,374 (41%)	1,505 (27%)
100th percentile	687 (12%)	716 (12%)	808 (14%)

Note. The numbers in parenthesis indicate the percentage of LIW that could have been caused by flashes with CC, relative to the 5,585, 5,731, and 5,634 analyzed wildfires with flashes candidates.

Moris (2022) and Schultz et al. (2019) in CONUS, we obtained that most wildfires (62%) are detected within less than 24 hr after the most probable lightning candidate. Furthermore, we obtained a significant number of lightning candidates (40%) more than 2 km away from the reported location of the fire. This proportion is considerably reduced to 26% when we select the distance between wildfires and flashes as the distance to the closest group detected by GLM (Figure 1d).

Table 1 shows the total number of LIW with at least one flash with CC candidate above a given percentile by using the coordinates of flashes ("Flash-based search") and the coordinates of groups ("Group-based search"). A maximum holdover of 14 days has been used, while the maximum distance imposed has been 10 km in both cases. Alternatively, a maximum distance of 25 km has also been used for the "Flash-based approach" case, since the position of the flashes has greater uncertainty than that of the groups. The minimum 0th percentile indicates that, for a fire, there is at least one flash with CC candidate within the sample of all candidate flashes, while the maximum 100th percentile indicates that the flash candidate with the maximum *A* index value is actually a flash with CC. On average, 185 lightning flashes per fire are assigned as possible candidates by using D_{max} = 10 km, T_{max} = 14 days, and the flashes coordinates, while this quantity descends to 10 and 2.5 when only lightning flashes with a proximity index *A* above the 95th and the 99th percentiles are selected, respectively. During the summer season in CONUS, the climatological ratio of CC flashes to total lightning is typically less than 10%. By setting the 95th and the 99th percentiles as the thresholds for identifying wildfires ignited by flashes with CC, we can ensure that the average number of flash candidates with CC per fire would be less than 1 if there is no correlation between CC and wildfires. These thresholds are chosen based on the assumption that a low ratio of CC flashes to total lightning reduces the likelihood of misclassifying wildfires as having been ignited by flashes with CC. The percentage of LIW produced by flashes with CC ranges between 12% for the 100th percentile and D_{max} = 10 km and 99% for the 0th percentile and D_{max} = 25 km by using the flashes coordinates. Finally, the percentage of LIW produced by flashes with CC ranges between 14% and 86% by using the groups coordinates.

3.1.2. Lightning Ignition Efficiency

Tables 2 and 3 show the total number of LIW, LIW associated with lightning with CC lasting more than 10 ms, total flashes, flashes with CC and LIE in different forest types and ecological regions by following the "Flash-based search," respectively. Wildfires are classified as ignited by a CC flash if there is at least one CC flash candidate with an *A* index about the 95th and the 99th percentiles, respectively. Lightning-induced wildfires are heterogeneously distributed over different forest types and ecological regions. Most of them took place over non-forest areas and pinyon juniper woodland, while the ecological regions with the highest occurrence of LIW were the Western Cordillera and the Cold Deserts.

The percentage of lightning-induced wildfires produced by flashes with CC are significantly higher than the ratio of flashes with CC to total flashes in all the analyzed forest types and ecological regions. Second, the total number of fires caused by lightning with CC is highly influenced by the percentile (e.g., 95th and 99th) of the *A* index value chosen as threshold. As a result, we encountered significant uncertainty in estimating the LIE of flashes with CC. Third, the uncertainty of the LIE of CG flashes is a consequence of the high variability (standard deviation) of the CG fraction over particular forest types and ecological regions. Fourth, total LIE, CG LIE, and LIE of flashes with CC show a relatively high variability over different forest types and ecological regions, while the variation in the percentage of flashes with CC is lower. Finally, when data from all the regions and forest types of the CONUS are pooled together, the global LIEs of lightning with CC using percentiles (95th and 99th) are greater than the average LIE of CG lightning, although within the interval of possible CG LIE defined by the standard deviation of the CG fraction.

Figure 2 shows a comparison between the LIE of CG flashes and the LIE of CC flashes in different forest types and ecological regions. We included error bars to take into consideration the effect of the standard deviation of the

Journal of Geophysical Research: Atmospheres
10.1029/2023JD038891

Table 2
LIE in Forest Types of CONUS

	Fires			Flashes			LIE			
Forest type	LIW	LIW (CC) 99th	LIW (CC) 95th	Total number of flashes	CG fraction ± σ	Flashes with CC to total flashes (%)	Total LIE × 10^{-3}	CG LIE × 10^{-3}	CC LIE (99th) × 10^{-3}	CC LIE (95th) × 10^{-3}
Non-forest	2,335	452 (19%)	823 (35%)	44,344,925	0.47 ± 0.32	11	0.05	0.11 [0.07–0.30]	0.10	0.18
Pinyon juniper woodland	933	162 (17%)	381 (41%)	497,241	0.33 ± 0.07	6	2	5.7 [4.8–7.0]	5.0	11.8
Ponderosa pine	793	184 (23%)	383 (48%)	265,834	0.28 ± 0.08	6	3	10.6 [8.2–15.2]	11.2	23.4
Douglas-fir	493	94 (19%)	138 (28%)	81,615	0.21 ± 0.08	10	6	29.1 [21.0–47.4]	11.1	16.4
Lodgepole pine	133	14 (11%)	29 (22%)	57,727	0.30 ± 0.09	8	2	7.6 [5.9–10.8]	2.9	6.1
Aspen	113	22 (19%)	39 (35%)	592,835	0.40 ± 0.11	7	0.2	0.47 [0.37–0.64]	0.52	0.93
Engelmann spruce/subalpine fir	108	13 (12%)	24 (22%)	37,855	0.27 ± 0.08	8	3	10.7 [8.3–15.3]	4.1	7.5
California mixed conifer	87	15 (17%)	21 (24%)	7,413	0.21 ± 0.07	8	12	55 [42–80]	24	34
Juniper woodland	84	9 (11%)	24 (29%)	23,315	0.31 ± 0.06	7	4	11.6 [9.7–14.4]	5.9	15.7
Loblolly pine	77	38 (49%)	59 (77%)	4,490,658	0.28 ± 0.02	9	0.02	0.061 [0.057–0.065]	0.10	0.15
Total	5,585	1,180 (21%)	2,218 (40%)	44,775,248	0.44 ± 0.26	8.7	0.12	0.28 [0.18–0.70]	0.30	0.57

Note. LIW is the total number of Lightning-Ignited Wildfires (LIW). LIW (CC) 99th and LIW (CC) 95th are the total number of LIW produced by lightning with CC according to the two criteria described in the text. The CG fraction is given together with the standard deviation over each forest type. The total, CG and CC lightning-ignition efficiency (LIE) for each forest type was calculated as the ratio of total Lightning-Ignited Wildfires (LIW) to total lightning, CG flashes and flashes with CC over the same ecological region, respectively. Only forest types with ≥2% of the total lightning-ignited wildfires are included here.

Journal of Geophysical Research: Atmospheres
10.1029/2023JD038891

Table 3
LIE in Ecological Regions of CONUS

	Fires			Flashes			LIE			
Ecological region	LIW	LIW (CC) 99th	LIW (CC) 95th	Total number of flashes	CG fraction ± σ	Flashes with CC to total flashes (%)	Total LIE × 10^{-3}	CG LIE × 10^{-3}	CC LIE (99th) × 10^{-3}	CC LIE (95th) × 10^{-3}
Western cordillera	1,957	319 (16%)	549 (28%)	758,850	0.33 ± 0.24	8	0.3	7.9 [4.6–30.4]	5.1	8.8
Cold deserts	1,598	208 (13%)	481 (30%)	1,039,041	0.30 ± 0.09	7	2	5.1 [3.9–7.1]	2.8	6.5
Upper gila mountains	671	176 (26%)	386 (58%)	538,836	0.37 ± 0.04	6	1	3.4 [3.1–3.8]	5.2	11.4
Southcentral semi-arid prairies	387	93 (24%)	167 (43%)	5,425,872	0.28 ± 0.06	6	0.07	0.26 [0.22–0.32]	0.28	0.51
Westcentral semi-arid prairies	345	83 (24%)	154 (45%)	2,335,319	0.26 ± 0.07	7	0.1	0.56 [0.43–0.78]	0.51	0.96
Mixed wood plains	189	28 (15%)	49 (26%)	1,468,676	0.43 ± 0.16	8	0.1	0.30 [0.22–0.48]	0.23	0.41
Mississippi alluvial and southeast USA coastal plains	166	93 (56%)	139 (84%)	4,731,225	0.29 ± 0.05	10	0.04	0.12 [0.11–0.14]	0.21	0.31
Southeastern USA plains	143	59 (41%)	92 (64%)	8,816,244	0.31 ± 0.06	9	0.02	0.05 [0.04–0.07]	0.08	0.12
Warm deserts	141	22 (16%)	49 (35%)	2,441,769	0.42 ± 0.34	7	0.06	0.14 [0.08–0.73]	0.13	0.28
Total	5,585	1,180 (21%)	2,218 (40%)	44,775,248	0.44 ± 0.26	8.7	0.12	0.28 [0.18–0.70]	0.30	0.57

Note. LIW is the total number of Lightning-Ignited Wildfires (LIW). LIW (CC) 99th and LIW (CC) 95th are the total number of LIW produced by lightning with CC according to the two criteria described in the text. The CG fraction is given together with the standard deviation over each ecological region. The total, CG and CC lightning-ignition efficiency (LIE) for each ecological region was calculated as the ratio of total Lightning-Ignited Wildfires (LIW) to total lightning, CG flashes and flashes with CC over the same ecological region, respectively. Only ecological regions with ≥2% of the total lightning-ignited wildfires are included here.

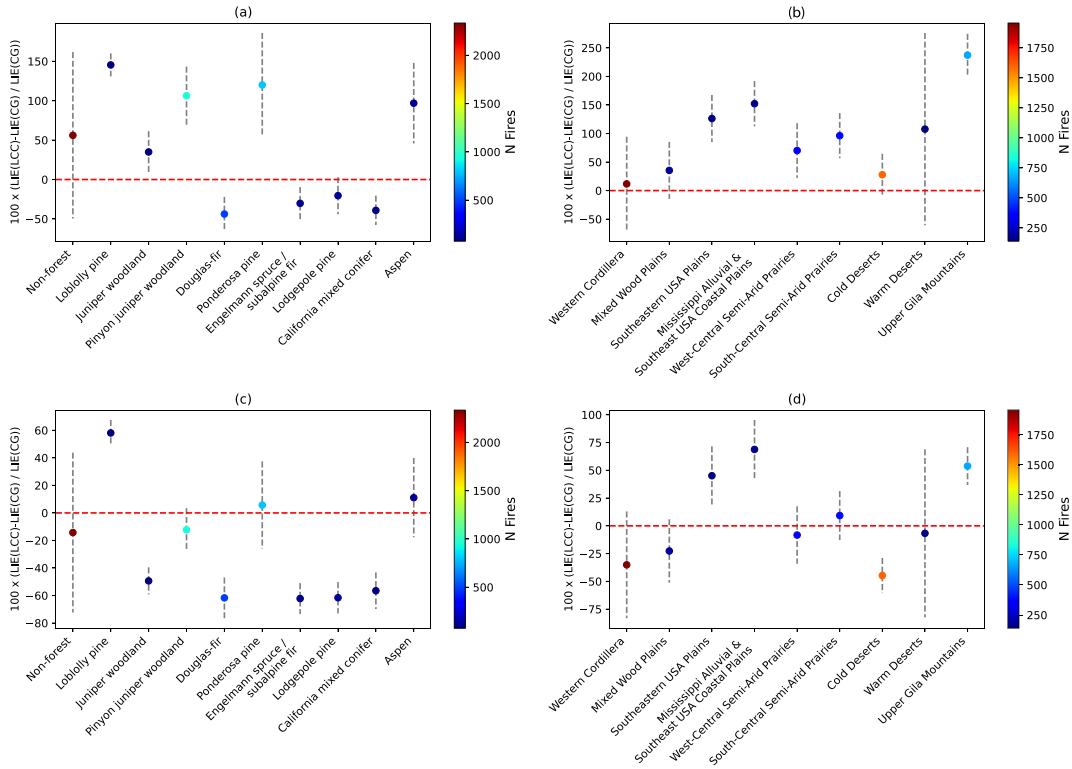

Figure 2. Differences (in %) between the Lightning Ignition Efficiency (LIE) of Cloud to Ground (CG) lightning and the LIE of flashes with Continuing Current (CC) in different forest types and ecological regions. The first and the second row show the comparison of the LIEs by assuming that lightning-induced wildfires are ignited by a flash with CC if there is at least one lightning candidate with CC with a proximity index A above the 95th percentile (a, b) and the 99th percentile (c, d), respectively. The colormap indicates the total number of lightning-induced wildfires in each forest type or ecological region. The error bar (gray dashed lines) represents the results by assuming the Intra-Cloud (IC) fraction $\pm \sigma$.

LIE of CG flashes. When using the 95th percentile threshold, the LIE of CC is higher than the LIE of CG flashes in the majority (but not all) of forest types and ecological regions (Figures 2a and 2b). However, this tendency is not clear when using the 99th percentile threshold (Figures 2c and 2d). If the error bars include the value 0, this indicated that the LIE of CC may not be higher (or lower) than the LIE of CG flashes for those forest types and ecological regions. In turn, we obtained high uncertainty in the comparison of the LIE of CC flashes and the LIE of CG lightning as a consequence of the high standard deviation of the CG fraction.

3.2. Optical and ELF Signature of a Lightning-Ignited Wildfire in the Valais

In this section, we analyzed the CC of a fire-igniting lightning flash recorded by a camera in the Valais (Switzerland) on 21 July 2021 between 21 and 22 hr (UTC-0) at 30 frames per second. Figure 3 shows four selected frames from the video. The advancing leader can be seen in the frame 124 before attachment to ground, while the frame 156 shows the most luminous phase of the return stroke after attachment. A second lightning flash behind the fire-igniting flash can be seen in the frame 169, about 0.5 s after the most luminous phase of the first flash. Finally, frame 200 shows the fire-igniting flash during the decay of its luminosity. The total duration of the flash luminosity was about 4 s, a long duration that could be influenced by the potential afterglow of pixels of the camera.

Table 4 shows all the strokes candidates for the fire-igniting flash detected by ENGLN and LINET between 21 and 22 hr and within 10 km of the position of the fire. The strokes labeled as * and # were simultaneously detected by both lightning location systems as CG, while the difference between them coincide with the timing between the two flashes detected in the video (lower that 0.5 s). Therefore, we concluded that the most probable stroke candidate for the recorded lightning-ignited wildfire in Valais is the positive CG stroke labeled as * and detected by ENGLN and LINET at about 21:23:26.21 hr.

Figure 3. Frames 124, 156, 169, and 200 extracted from the video of a lightning-ignited wildfire in the Valais (Switzerland) (Berckum et al., 2023). The two detected lightning channels are labeled with the symbols * and #, respectively.

The magnetic field reported by the ELF sensor associated with the stroke candidate is plotted in Figure 4 together with the temporal evolution of the luminosity. The luminosity is extracted from a single pixel located in the channel of the flash that produces the fire. This pixel has coordinates (200, 160), and it is positioned at half the height of the channel and radially centered. Because the exact absolute timing of the video is not known, the temporal evolution of the luminosity has been manually synchronized with the ELF signal. The temporal evolution of the magnetic field indicates the existence of a CC lasting about 400 ms, while the duration of the luminosity is significantly larger (between 2 and 4 s). In turn, there are several coincidences between the peaks of the magnetic and the optical signals. On the other hand, we obtained a CMC of 188 C km. In summary, the analysis of the optical and the ELF radio signal of this event confirms that the recorded fire-igniting flash had a long CC.

4. Discussion

4.1. Lightning Candidates

A daily cycle emerges in the distribution of the holdover (Figure 1b), probably, as a consequence of the diurnal cycle of temperature and relative humidity (Pérez-Invernón, Huntrieser, & Moris, 2022; Pineda et al., 2014; Pineda & Rigo, 2017). Contrary to Pérez-Invernón, Huntrieser, and Moris (2022) and Schultz et al. (2019), we obtained a significant number of lightning candidates (40%) more than 2 km away from the reported location of the fire (Figure 1c). The high frequency of distances above 2 km may be due to the difference between the point where the lightning strikes the ground and the flash location calculated as the position of the centroid of the groups weighted by their energy. The frequency of distances above 2 km is significantly reduced from 40% to 26% when we consider the distance between a fire and a flash as the distance to the closest group reported by GLM.

4.2. Role of Flashes With CC in Igniting Lightning-Induced Wildfires

The role of continuing currents in LIW was previously suggested by field and laboratory observations (Feng et al., 2019; McEachron & Hagenguth, 1942; H. Zhang et al., 2021). However, quantifying this role at a larger scale was not possible until recently due to the low detection efficiency of lightning location systems for continuing currents and the uncertainty related to the identification of the lightning causing the reported wildfires. Using continuous optical measurements from geostationary orbit by GLM over CONUS, Pérez-Invernón et al. (2023) suggested that continuing currents could play a significant role in the ignition of wildfires. In this work, we extended the analysis of Pérez-Invernón et al. (2023) by calculating the LIE of total, CG and lightning with CC in different forest types and ecological regions. We used the method developed by Fairman and Bitzer (2022) to identify continuing currents from optical measurements of GLM lasting more than 10 ms and the wildfire data reported by Short (2021) and Wright et al. (2011) between June and August 2018 over CONUS.

We found that the global LIE of flashes with CC lasting more than 10 ms is higher than the averaged LIE of CG flashes over CONUS, indicating that models of lightning-induced wildfire risk could benefit from including information on flashes with CC observed from space. However, the results on LIEs vary greatly with the threshold of percentile used to select lightning candidates (Figure 2). In addition, we found that the LIE varies

Table 4
Strokes Candidates (Intra-Cloud [IC] or Cloud to Ground [CG]) for the Fire-Igniting Lightning Recorded in Valais

Lightning location system (LSS)	ID	Timestamp	Latitude	Longitude	Peak current (kA)	Type	Reference in Figure 3
ENGLN	1	2020-07-21 21:20:53.378350019	46.2918	7.5414	−13.359	IC	
	2	2020-07-21 21:20:53.244531155	46.29827	7.627370	5.498	IC	
	3	2020-07-21 21:20:53.260302544	46.31427	−7.4410	5.498	IC	
	4	2020-07-21 21:23:26.210532188	46.29874	−7.64204	46.582	CG	*
	5	2020-07-21 21:23:26.397774220	46.27681	−7.6055	−5.884	CG	#
	6	2020-07-21 21:23:26.503840923	46.25791	−7.61851	−5.122	CG	
	7	2020-07-21 21:23:26.526084185	46.25764	−7.60186	−4.469	CG	
LINET	1	2020-07-21 21:18:45.7141833	46.2688	7.6258	31.5	CG	
	2	2020-07-21 21:20:53.3766246	46.3072	7.654	10.2	CG	
	3	2020-07-21 21:23:26.210559	46.2984	7.6299	51.4	CG	*
	4	2020-07-21 21:23:26.3978106	46.2419	7.635	−4.1	CG	#
	5	2020-07-21 21:23:26.4189219	46.2496	7.6362	−4.6	IC	
	6	2020-07-21 21:23:26.5038673	46.2417	7.6361	−3.3	CG	
	7	2020-07-21 21:29:06.2848312	46.2348	7.5024	2.6	CG	

Note. The labels * and # indicate the strokes candidates for the lightning channels showed in Figure 3.

importantly with the forest type and the ecological region (Tables 2 and 3), which agrees with previous studies (e.g., Pérez-Invernón, Huntrieser, and Moris, 2022; Pineda et al., 2022; Schultz et al., 2019). More data are needed to confirm our results, such as larger samples of LIW and meteorological variables across different regions.

D. Fuquay et al. (1972) reported simultaneous observations of 11 fire-igniting lightning by optical cameras and ELF radio sensors, confirming the presence of continuing currents. Here, we combined the optical signal of a lightning discharge starting a wildfire in the Alps from a ground-based camera with lightning measurements provided by two lightning location systems (ENGLN and LINET) and an ELF radio sensor. The duration of both the optical and the ELF radio signature suggests the presence of a long-lasting CC in the lightning flash that ignited the wildfire, followed by possible M-components produced by the interaction between an in-cloud advancing leader and the main cloud-to-ground channel (Tran & Rakov, 2019). The luminosity indicates that the channel does not turn off after 400 ms, suggesting that the ELF radio sensor would miss the decay of the CC. The consecutive peaks in ELF and the luminosity could possibly be attributed to M-components (Cai et al., 2022; Rakov et al., 1995) that would transfer more charge than the CC (Y. Zhang et al., 2016), which would allow for the ELF radio sensor to again detect it, as reported by Lapierre et al. (2014) for a flash with CC in New Mexico. Systematic differences in the total duration of the luminosity and the ELF radio signal of flashes with CC has been previously reported by several authors (e.g., Kohlmann et al., 2022; Saba et al., 2006). For example, Kohlmann et al. (2022) reported that the duration of the CC detected by the ELF radio sensor are between 10% and 69% shorter than in the videos. They suggested a number of reasons that could explain these differences, including a possible overdub of the E-field change, transfer of charge produced by the leader or a chemical afterglow producing optical emissions. The obtained CMC (188 C km) was higher than in typical lightning discharges and is in agreement with the CMC reported by D. Fuquay et al. (1972) in western Montana forests. In conclusion, the analysis of this single case study supports our results at a large spatial scale obtained from the analysis of GLM lightning measurements over the CONUS, suggesting that flashes with CC are more likely to cause wildfires.

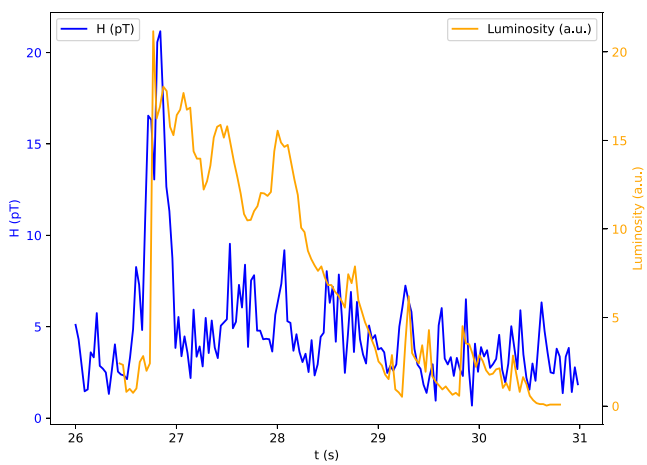

Figure 4. Temporal evolution of the luminosity of a pixel located at the center of the lightning channel of the video showed in Figure 3 (orange line) and the magnetic field Extremely Low Frequency signature (blue line). The units of the magnetic field are pT, while the luminosity is plotted in arbitrary units in the same *y*-axis as the magnetic field.

4.3. Limits of the Study

Here, we report a higher probability of wildfire ignition by flashes with CC lasting more than 10 ms than by total and CG lightning. However, several aspects limit the interpretation of our findings. For instance, the uncertainty related to one-to-one relationship between wildfires and lightning flashes remains high. We used a proximity index that combines the holdover time and distance between reported lightning and fires to search for the most probable lightning candidates. The large amount of lightning flashes detected by GLM with positive values of the proximity index (see Table 1) introduces a substantial uncertainty in the determination of the most probable lightning candidate. This uncertainty is enhanced by the difficulties in distinguishing between IC and CG flashes from space (Ringhausen et al., 2021). In addition, the misclassification of continuing currents may introduce more uncertainty, given that we cannot rule out the possibility that some IC lightning producing long-lasting optical emissions are also classified as CG lightning with CC (Fairman & Bitzer, 2022).

On the other hand, under conservative scenarios for selecting lightning candidates (=10 km and 95–100th percentiles of the proximity index A), we found that 12%–40% of all the LIW may have been caused by a lightning event with CC. Therefore, our results suggest that a high proportion of wildfires may actually be caused by lightning without CC given that these non-CC lightning are simply much more common. Consequently, we cannot exclude the possibility that most of the lightning-induced wildfires are ignited by lightning discharges without a CC phase.

The high uncertainty levels related to both the selection of candidate lightning as well as the fraction of CG flashes complicate the comparison between values of LIE CC and LIE CG. First, the percentiles used to decide how many fires were produced by lightning with CC (e.g., 95th or 99th) have a strong influence on LIE CC (Table 2). On the other side, the spatial variability in the climatology of CG fraction results generally in high values of standard deviation of CG fraction, and consequently in broad ranges of potential values of LIE CG (Table 2). Future research could apply better estimations on the fraction of CG flashes, for example, with the support of auxiliary lightning data from the specific period of study (e.g., summer 2018 in this research).

Finally, the prolonged duration of the lightning-induced wildfire in the Alps suggests that the CC duration could last for several hundred milliseconds (LCC lightning), whereas our current classification of lightning with CC from GLM measurements includes all flashes with a CC lasting more than 10 milliseconds. This difference in duration may be of relevance for estimating the LIE of lightning with CC. Hence, developing a new classification of LCC lightning based on GLM measurements could be valuable for studying the impact of CC duration on ignition probability.

5. Conclusions

The main conclusions of this work are:

1. The probability of wildfire ignition by CG lightning is larger for flashes with CC. In particular, we found that approximately 12%–14% of lightning-induced wildfires are attributed to flashes with CC as the most probable lightning candidate, whereas the overall occurrence of flashes with CC among all lightning strikes is approximately 10%.
2. The significant variation in the LIE of lightning with CC across different forest types and ecological regions suggests that other factors, such as wildland fuel characteristics and fire-related meteorological conditions, exert a substantial influence.
3. The detailed analysis of one single lightning-ignited fire in the Alps by combining optical, VLF, and ELF measurements confirms the presence of a LCC in the lightning discharge that started the fire.
4. The holdover time and spatial distance between wildfires and lightning candidates identified from the GLM groups show remarkable similarities from the stroke and flash data typically observed in lightning networks. This novel finding holds significant value for ecological studies.

Our results on the role of CC lightning in the ignition of wildfires indicates that parameterizations of flashes with CC in atmospheric models (Pérez-Invernón, Huntrieser, Jöckel, & Gordillo-Vázquez, 2022) together with information on forest types and their fuel characteristics may improve the forecasting of lightning-induced wildfires. More data on wildfire and lightning detection across the field of view of GLM aboard the GOES-17 satellite will provide new information about the role of flashes with CC in the Americas. Similarly, the MTG-LI will

provide new measurements of flashes with CC over Europe and Africa from 2023, contributing to extend the analysis at a global scale.

Data Availability Statement

The GLM lightning data sets may be obtained from NOAA via their CLASS service (GOES-R Series Program, 2019). The data of LIW used in this study are freely available (Glasgow et al., 2023). Forest type data can be freely downloaded (USDA Forest Service & GTAC, 2009). Ecoregion data can be freely downloaded (EPA, 2023). ENGLN lightning data are available after using the contact form of Earth Networks (https://get.earthnetworks.com/contactus). LINET lightning data are available after using the contact form of Nowcast GmbH (https://www.nowcast.de/en/company/contact/). The video of the lightning-induced wildfire in the Valais (Switzerland) can be downloaded from Berckum et al. (2023).

Acknowledgments

The authors would like to thank Noah Michael Berckum, who recorded the video of the lightning-induced wildfires in the Valais. In addition, the authors thank NOAA for providing GLM lightning data, Earth Networks and Nowcast GmbH for providing lightning measurements and the National Interagency Fire Center for providing lightning-ignited wildfire data. FJPI acknowledges the sponsorship provided by the Federal Ministry for Education and Research of Germany through the Alexander von Humboldt Foundation, the sponsorship provided by Junta de Andalucía under Grant POST-DOC-21-0005. The project that gave rise to these results received the support of a fellowship from "la Caixa" Foundation (ID 100010434). The fellowship code is LCF/BQ/PI22/11910026 (FJPI). JVM acknowledges the support from a postdoctoral fellowship funded by the Government of Asturias (Spain) through FICYT (AYUD/2021/58534). The work of MF is was sponsored by the Royal Society (UK) Grant NMG/R1/180252 and the Natural Environment Research Council (UK) under Grants NE/L012669/1 and NE/H024921/1. Additionally, this work was supported by the Spanish Ministry of Science and Innovation, under projects PID2019-109269RB-C43 (F.J.P.I. and F.J.G.V) and PID2022-136348NB-C31 (F.J.P.I. and F.J.G.V) funded by MCIN/AEI/10.13039/501100011033 and "ERDF A way of making Europe." FJPI and FJGV acknowledge financial support from the State Agency for Research of the Spanish MCIU through the "Center of Excellence Severo Ochoa" from the Grant CEX2021-001131-S funded by MCIN/AEI/10.13039/501100011033.

References

Adachi, T., Cummer, S. A., Li, J., Takahashi, Y., Hsu, R.-R., Su, H.-T., et al. (2009). Estimating lightning current moment waveforms from satellite optical measurements. *Geophysical Research Letters*, *36*(18), L18808. https://doi.org/10.1029/2009GL039911

Akagi, S. K., Yokelson, R. J., Wiedinmyer, C., Alvarado, M. J., Reid, J. S., Karl, T., et al. (2011). Emission factors for open and domestic biomass burning for use in atmospheric models. *Atmospheric Chemistry and Physics*, *11*(9), 4039–4072. https://doi.org/10.5194/acp-11-4039-2011

Anderson, K. (2002). A model to predict lightning-caused fire occurrences. *International Journal of Wildland Fire*, *11*(4), 163–172. https://doi.org/10.1071/wf02001

Berckum, N. M., Pérez-Invernón, F. J., Moris, J. V., Gordillo-Vázquez, F. J., Füllekrug, M., Pezzatti, G. B., et al. (2023). Lightning-induced wildfire in the Valais (Switzerland) [Video]. *Zenodo*. https://doi.org/10.5281/zenodo.7983783

Betz, H. D., Schmidt, K., Laroche, P., Blanchet, P., Oettinger, W. P., Defer, E., et al. (2009). LINET - An international lightning detection network in Europe. *Atmospheric Research*, *91*(2–4), 564–573. https://doi.org/10.1016/j.atmosres.2008.06.012

Bitzer, P. M. (2017). Global distribution and properties of continuing current in lightning. *Journal of Geophysical Research: Atmospheres*, *122*(2), 1033–1041. https://doi.org/10.1002/2016JD025532

Bitzer, P. M., Burchfield, J. C., & Christian, H. J. (2016). A Bayesian approach to assess the performance of lightning detection systems. *Journal of Atmospheric and Oceanic Technology*, *33*(3), 563–578. https://doi.org/10.1175/JTECH-D-15-0032.1

Cai, L., Hu, Q., Zhou, M., Tian, R., Su, R., Fan, Y., & Wang, J. (2022). Characteristics of continuing current waveforms and M-component parameters in triggered lightning. *Journal of Geophysical Research: Atmospheres*, *127*(23), e2022JD036878. https://doi.org/10.1029/2022JD036878

Calef, M. P., Varvak, A., & McGuire, A. D. (2017). Differences in human versus lightning fires between urban and rural areas of the boreal forest in interior Alaska. *Forests*, *8*(11), 422. https://doi.org/10.3390/f8110422

Chen, Y., Romps, D. M., Seeley, J. T., Veraverbeke, S., Riley, W. J., Mekonnen, Z. A., & Randerson, J. T. (2021). Future increases in Arctic lightning and fire risk for permafrost carbon. *Nature Climate Change*, *11*(5), 404–410. https://doi.org/10.1038/s41558-021-01011-y

Commission for Environmental Cooperation. (1997). *Ecological regions of North America: Toward a common perspective*. Commission for Environmental Cooperation. 71 p. map (scale 1:12,500,000) (Revised 2006).

Coogan, S. C., Cai, X., Jain, P., & Flannigan, M. D. (2020). Seasonality and trends in human-and lightning-caused wildfires ≥ 2 ha in Canada, 1959–2018. *International Journal of Wildland Fire*, *29*(6), 473–485. https://doi.org/10.1071/WF19129

EPA. (2023). EPA United States Environmental Protection Agency. Ecoregions of North America [Dataset]. Retrieved from https://www.epa.gov/eco-research/ecoregions-north-america

Fairman, S. I., & Bitzer, P. M. (2022). The detection of continuing current in lightning using the Geostationary Lightning Mapper. *Journal of Geophysical Research: Atmospheres*, *127*(5), e2020JD033451. https://doi.org/10.1029/2020JD033451

Feng, J., Shen, H., & Liang, D. (2019). Investigation of lightning ignition characteristics based on an impulse current generator. *Ecology and Evolution*, *9*(24), 14234–14243. https://doi.org/10.1002/ece3.5855

Füllekrug, M. (2000). Dispersion relation for spherical electromagnetic resonances in the atmosphere. *Physics Letters A*, *275*(1–2), 80–89. https://doi.org/10.1016/S0375-9601(00)00549-1

Füllekrug, M., & Constable, S. (2000). Global triangulation of intense lightning discharges. *Geophysical Research Letters*, *27*(3), 333–336. https://doi.org/10.1029/1999GL003684

Füllekrug, M., Ignaccolo, M., & Kuvshinov, A. (2006). Stratospheric Joule heating by lightning continuing current inferred from radio remote sensing. *Radio Science*, *41*(02), 1–5. https://doi.org/10.1029/2006RS003472

Fuquay, D., Taylor, A., Hawe, R., & Schmid, C., Jr. (1972). Lightning discharges that caused forest fires. *Journal of Geophysical Research*, *77*(12), 2156–2158. https://doi.org/10.1029/JC077i012p02156

Fuquay, D. M., Baughman, R., Taylor, A., & Hawe, R. (1967). Characteristics of seven lightning discharges that caused forest fires. *Journal of Geophysical Research*, *72*(24), 6371–6373. https://doi.org/10.1029/JZ072i024p06371

Glasgow, L. S., Wright, D. K., & Sutherland, E. K. (2023). Coram Experimental Forest 15 minute streamflow data [Dataset]. Forest Service Research Data Archive. https://doi.org/10.2737/RDS-2011-0019

GOES-R Series Program. (2019). NOAA GOES-R Series Geostationary Lightning Mapper (GLM) level 0 data [Dataset]. https://doi.org/10.25921/qc2r-ps67

Goodman, S. J., Blakeslee, R. J., Koshak, J. M., Mach, D., Bailey, J., Buechler, D., et al. (2013). The GOES-R geostationary lightning mapper (GLM). *Atmospheric Research*, *125*, 34–49. https://doi.org/10.1016/j.atmosres.2013.01.006

Hantson, S., Andela, N., Goulden, M. L., & Randerson, J. T. (2022). Human-ignited fires result in more extreme fire behavior and ecosystem impacts. *Nature Communications*, *13*(1), 2717. https://doi.org/10.1038/s41467-022-30030-2

Huntrieser, H., Lichtenstern, M., Scheibe, M., Aufmhoff, H., Schlager, H., Pucik, T., et al. (2016). Injection of lightning-produced NO_x, water vapor, wildfire emissions, and stratospheric air to the UT/LS as observed from DC3 measurements. *Journal of Geophysical Research: Atmospheres*, *121*(11), 6638–6668. https://doi.org/10.1002/2015JD024273

Justice, C., Giglio, L., Korontzi, S., Owens, J., Morisette, J., Roy, D., et al. (2002). The MODIS fire products. *Remote Sensing of Environment*, *83*(1–2), 244–262. https://doi.org/10.1016/s0034-4257(02)00076-7

Kieu, N., Gordillo-Vázquez, F. J., Passas, M., Sánchez, J., & Pérez-Invernón, F. J. (2021). High-speed spectroscopy of lightning-like discharges: Evidence of molecular optical emissions. *Journal of Geophysical Research: Atmospheres*, *126*(11), e2021JD035016. https://doi.org/10.1029/2021JD035016

Kohlmann, H., Schulz, W., & Rachidi, F. (2022). Estimation of charge transfer during long continuing currents in natural downward flashes using single-station e-field measurements. *Journal of Geophysical Research: Atmospheres*, *127*(6), e2021JD036197. https://doi.org/10.1029/2021JD036197

Komarek, E. (1964). The natural history of lightning. In *Proceedings of the tall timbers fire ecology conference* (Vol. 3, pp. 139–183).

Krause, A., Kloster, S., Wilkenskjeld, S., & Paeth, H. (2014). The sensitivity of global wildfires to simulated past, present, and future lightning frequency. *Journal of Geophysical Research: Biogeosciences*, *119*(3), 312–322. https://doi.org/10.1002/2013JG002502

Lapierre, J. L., Sonnenfeld, R. G., Edens, H. E., & Stock, M. (2014). On the relationship between continuing current and positive leader growth. *Journal of Geophysical Research: Atmospheres*, *119*(22), 12–479. https://doi.org/10.1002/2014JD022080

Larjavaara, M., Pennanen, J., & Tuomi, T. (2005). Lightning that ignites forest fires in Finland. *Agricultural and Forest Meteorology*, *132*(3–4), 171–180. https://doi.org/10.1016/j.agrformet.2005.07.005

Latham, D., & Williams, E. (2001). Lightning and forest fires. In *Forest fires* (1st ed., pp. 375–418). Elsevier.

Mach, D. M., Christian, H. J., Blakeslee, R. J., Boccippio, D. J., Goodman, S. J., & Boeck, W. L. (2007). Performance assessment of the optical transient detector and lightning imaging sensor. *Journal of Geophysical Research*, *112*(D9), D09210. https://doi.org/10.1029/2006JD007787

Marchand, M., Hilburn, K., & Miller, S. D. (2019). Geostationary Lightning Mapper and Earth Networks lightning detection over the contiguous United States and dependence on flash characteristics. *Journal of Geophysical Research: Atmospheres*, *124*(21), 11552–11567. https://doi.org/10.1029/2019JD031039

McEachron, K., & Hagenguth, J. (1942). Effect of lightning on thin metal surfaces. *IEEE Transactions on Communications*, *61*(8), 559–564. https://doi.org/10.1109/T-AIEE.1942.5058563

Medici, G., Cummins, K. L., Cecil, D. J., Koshak, W. J., & Rudlosky, S. D. (2017). The intracloud lightning fraction in the contiguous United States. *Monthly Weather Review*, *145*(11), 4481–4499. https://doi.org/10.1175/MWR-D-16-0426.1

Montanyà, J., López, J., van der Velde, O., Sola, G., Romero, D., Morales, C., et al. (2022). Potential use of space-based lightning detection in electric power systems. *Electric Power Systems Research*, *213*, 108730. https://doi.org/10.1016/j.epsr.2022.108730

Montanyà, J., López, J. A., Morales Rodriguez, C. A., van der Velde, O. A., Fabró, F., Pineda, N., et al. (2021). A simultaneous observation of lightning by ASIM, Colombia-Lightning Mapping Array, GLM, and ISS-LIS. *Journal of Geophysical Research: Atmospheres*, *126*(6), e2020JD033735. https://doi.org/10.1029/2020JD033735

Moris, J. V., Álvarez-Álvarez, P., Conedera, M., Dorph, A., Hessilt, T. D., Hunt, H. G., et al. (2023). A global database on holdover time of lightning-ignited wildfires. *Earth System Science Data Discussions*, *15*, 1151–1163, https://doi.org/10.5194/essd-15-1151-2023

Moris, J. V., Conedera, M., Nisi, L., Bernardi, M., Cesti, G., & Pezzatti, G. B. (2020). Lightning-caused fires in the Alps: Identifying the igniting strokes. *Agricultural and Forest Meteorology*, *290*, 107990. https://doi.org/10.1016/j.agrformet.2020.107990

Musur, M., & Beggan, C. (2019). Seasonal and solar cycle variation of Schumann resonance intensity and frequency at Eskdalemuir Observatory, UK. *Sun and Geosphere*, *14*(1), 81–86. https://doi.org/10.31401/SunGeo.2019.01.11

Nag, A., Murphy, M. J., Schulz, W., & Cummins, K. L. (2015). Lightning locating systems: Insights on characteristics and validation techniques. *Earth and Space Science*, *2*(4), 65–93. https://doi.org/10.1002/2014EA000051

Orville, R. E. (1968). Spectrum of the lightning stepped leader. *Journal of Geophysical Research*, *73*(22), 6999–7008. https://doi.org/10.1029/JB073i022p06999

Pérez-Invernón, F. J., Gordillo-Vázquez, F. J., Huntrieser, H., & Jöckel, P. (2023). Variation of lightning-ignited wildfire patterns under climate change. *Nature Communications*, *14*(1), 739. https://doi.org/10.1038/s41467-023-36500-5

Pérez-Invernón, F. J., Gordillo-Vázquez, F. J., & Luque, A. (2016). On the electrostatic field created at ground level by a halo. *Geophysical Research Letters*, *43*(13), 7215–7222. https://doi.org/10.1002/2016GL069590

Pérez-Invernón, F. J., Gordillo-Vázquez, F. J., Passas-Varo, M., Neubert, T., Chanrion, O., Reglero, V., & Østgaard, N. (2022). Multispectral optical diagnostics of lightning from space. *Remote Sensing*, *14*(9), 2057. https://doi.org/10.3390/rs14092057

Pérez-Invernón, F. J., Huntrieser, H., Erbertseder, T., Loyola, D., Valks, P., Liu, S., et al. (2022). Quantification of lightning-produced NO_x over the Pyrenees and the Ebro Valley by using different TROPOMI-NO_2 and cloud research products. *Atmospheric Measurement Techniques*, *15*(11), 3329–3351. https://doi.org/10.5194/amt-15-3329-2022

Pérez-Invernón, F. J., Huntrieser, H., Jöckel, P., & Gordillo-Vázquez, F. J. (2022). A parameterization of long-continuing-current (LCC) lightning in the lightning submodel LNOX (version 3.0) of the Modular Earth Submodel System (MESSy, version 2.54). *Geoscientific Model Development*, *15*(4), 1545–1565. https://doi.org/10.5194/gmd-15-1545-2022

Pérez-Invernón, F. J., Huntrieser, H., & Moris, J. V. (2022). Meteorological conditions associated with lightning ignited fires and long-continuing-current lightning in Arizona, New Mexico and Florida. *Fire*, *5*(4), 96. https://doi.org/10.3390/fire5040096

Pérez-Invernón, F. J., Huntrieser, H., Soler, S., Gordillo-Vázquez, F. J., Pineda, N., Navarro-González, J., et al. (2021). Lightning-ignited wildfires and long-continuing-current lightning in the Mediterranean basin: Preferential meteorological conditions. *Atmospheric Chemistry and Physics*, *21*(23), 1–43. https://doi.org/10.5194/acp-21-17529-2021

Peterson, M. (2019). Research applications for the Geostationary Lightning Mapper operational lightning flash data product. *Journal of Geophysical Research: Atmospheres*, *124*(17–18), 10205–10231. https://doi.org/10.1029/2019JD031054

Peterson, M., & Mach, D. (2022). The illumination of thunderclouds by lightning: 4. Volumetric thunderstorm imagery. *Earth and Space Science*, *9*(1), e2021EA001945. https://doi.org/10.1029/2021EA001945

Pezzatti, G. B., Bertogliati, M., Gache, S., Reinhard, M., & Conedera, M. (2019). Swissfire: Technisch modernisiert und dank Archivrecherchen inhaltlich erweitert. *Schweizerische Zeitschrift fur Forstwesen*, *170*(5), 234–241. https://doi.org/10.3188/szf.2019.0234

Pineda, N., Altube, P., Alcasena, F. J., Casellas, E., San Segundo, H., & Montanyà, J. (2022). Characterising the holdover phase of lightning-ignited wildfires in Catalonia. *Agricultural Meteorology*, *324*, 109111. https://doi.org/10.1016/j.agrformet.2022.109111

Pineda, N., Montanyà, J., & Van der Velde, O. A. (2014). Characteristics of lightning related to wildfire ignitions in Catalonia. *Atmospheric Research*, *135*, 380–387. https://doi.org/10.1016/j.atmosres.2012.07.011

Pineda, N., & Rigo, T. (2017). The rainfall factor in lightning-ignited wildfires in Catalonia. *Agricultural and Forest Meteorology*, *239*, 249–263. https://doi.org/10.1016/j.atmosres.2012.07.011

Podur, J., Martell, D. L., & Csillag, F. (2003). Spatial patterns of lightning-caused forest fires in Ontario, 1976–1998. *Ecological Modelling*, *164*(1), 1–20. https://doi.org/10.1016/S0304-3800(02)00386-1

Pyne, S. J., Andrews, P. L., Laven, R. D., & Cheney, N. (1998). Introduction to wildland fire. *Forestry*, *71*(1), 82. https://doi.org/10.1093/forestry/71.1.82

Rakov, V. A., Thottappillil, R., Uman, M. A., & Barker, P. P. (1995). Mechanism of the lightning M component. *Journal of Geophysical Research*, *100*(D12), 25701–25710. https://doi.org/10.1029/95JD01924

Rakov, V. A., & Uman, M. A. (2003). In V. A. Rakov & M. A. Uman (Eds.), *Lightning physics and effects*. Cambridge University Press.

Ringhausen, J., Bitzer, P., Koshak, W., & Mecikalski, J. (2021). Classification of GLM flashes using random forests. *Earth and Space Science*, *8*(11), e2021EA001861. https://doi.org/10.1029/2021EA001861

Rodrigues, M., Camprubí, À. C., Balaguer-Romano, R., Megía, C. J. C., Castañares, F., Ruffault, J., et al. (2023). Drivers and implications of the extreme 2022 wildfire season in southwest Europe. *Science of the Total Environment*, *859*, 160320. https://doi.org/10.1016/j.scitotenv.2022.160320

Rudlosky, S. D., Peterson, M. J., & Kahn, D. T. (2017). GLD360 performance relative to TRMM LIS. *Journal of Atmospheric and Oceanic Technology*, *34*(6), 1307–1322. https://doi.org/10.1175/JTECH-D-16-0243.1

Ruefenacht, B., Finco, M., Nelson, M., Czaplewski, R., Helmer, E., Blackard, J., et al. (2008). Conterminous US and Alaska forest type mapping using forest inventory and analysis data. *Photogrammetric Engineering & Remote Sensing*, *74*(11), 1379–1388. https://doi.org/10.14358/PERS.74.11.1379

Saba, M., Pinto, O., Jr., & Ballarotti, M. (2006). Relation between lightning return stroke peak current and following continuing current. *Geophysical Research Letters*, *33*(23), L23807. https://doi.org/10.1029/2006GL027455

Schultz, C. J., Nauslar, N. J., Wachter, J. B., Hain, C. R., & Bell, J. R. (2019). Spatial, temporal and electrical characteristics of lightning in reported lightning-initiated wildfire events. *Fire*, *2*(2), 18. https://doi.org/10.3390/fire2020018

Short, K. C. (2021). *Spatial wildfire occurrence data for the United States, 1992-2018 [fpa_fod_20210617]* (5th ed.). Forest Service Research Data Archive. https://doi.org/10.2737/RDS-2013-0009.5

Stuhlmann, R., Rodriguez, A., Tjemkes, S., Grandell, J., Arriaga, A., Bézy, J.-L., et al. (2005). Plans for EUMETSAT's Third Generation Meteosat geostationary satellite programme. *Advances in Space Research*, *36*(5), 975–981. https://doi.org/10.1016/j.asr.2005.03.091

Tran, M., & Rakov, V. (2019). An advanced model of lightning M-component. *Journal of Geophysical Research: Atmospheres*, *124*(4), 2296–2317. https://doi.org/10.1029/2018JD029604

USDA Forest Service, & GTAC. (2009). Conterminous U.S. and Alaska forest type mapping using forest inventory and analysis data [Dataset]. SDA Forest Service - Forest Inventory and Analysis (FIA) Program and Geospatial Technology and Applications Center (GTAC). Retrieved from https://data.fs.usda.gov/geodata/rastergateway/forest_type/index.php

Wotton, B., & Martell, D. L. (2005). A lightning fire occurrence model for Ontario. *Canadian Journal of Forest Research*, *35*(6), 1389–1401. https://doi.org/10.1139/x05-071

Wright, D. K., Glasgow, L. S., McCaughey, W. W., & Sutherland, E. K. (2011). *Coram experimental forest 15 minute streamflow data*. U.S. Department of Agriculture, Forest Service, Rocky Mountain Research Station. https://doi.org/10.2737/RDS-2011-0019

Yang, J., Zhang, Z., Wei, C., Lu, F., & Guo, Q. (2017). Introducing the new generation of Chinese geostationary weather satellites, Fengyun-4. *Bulletin of the American Meteorological Society*, *98*(8), 1637–1658. https://doi.org/10.1175/BAMS-D-16-0065.1

Zhang, H., Qiao, Y., Chen, H., Liu, N., Zhang, L., & Xie, X. (2021). Experimental study on flaming ignition of pine needles by simulated lightning discharge. *Fire Safety Journal*, *120*, 103029. https://doi.org/10.1016/j.firesaf.2020.103029

Zhang, Y., Zhang, Y., Xie, M., Zheng, D., Lu, W., Chen, S., & Yan, X. (2016). Characteristics and correlation of return stroke, M component and continuing current for triggered lightning. *Electric Power Systems Research*, *139*, 10–15. (Progress on Lightning Research and Protection Technologies). https://doi.org/10.1016/j.epsr.2015.11.024

Zheng, B., Ciais, P., Chevallier, F., Yang, H., Canadell, J. G., Chen, Y., et al. (2023). Record-high CO_2 emissions from boreal fires in 2021. *Science*, *379*(6635), 912–917. https://doi.org/10.1126/science.ade0805

Zhu, Y., Rakov, V. A., Mallick, S., & Tran, M. D. (2015). Characterization of negative cloud-to-ground lightning in Florida. *Journal of Atmospheric and Solar-Terrestrial Physics*, *136*, 8–15. https://doi.org/10.1016/j.jastp.2015.08.006

Zhu, Y., Stock, M., Lapierre, J., & DiGangi, E. (2022). Upgrades of the earth networks total lightning network in 2021. *Remote Sensing*, *14*(9), 2209. https://doi.org/10.3390/rs14092209